

Structure and low-temperature thermal relaxation of ion-implanted germanium.

C.J. Glover^a, M.C. Ridgway^a, K.M Yu^b, G.J. Foran^c,
C. Clerc^d, J.L Hansen^e and A. Nylandsted-Larsen^e.

^aResearch School of Physical Sciences and Engineering, Australian National University, Canberra, Australia, ^bMaterials Science Division, Lawrence Berkeley National Laboratory, Berkeley, USA, ^cAustralian Nuclear Science and Technology Organisation, Menai, Australia, ^dCentre National de Recherche Scientifique, Orsay, France, ^eInstitute of Physics and Astronomy, Aarhus University, Aarhus, Denmark.

The structure of implantation-induced damage in Ge has been investigated using high resolution extended X-ray absorption fine structure spectroscopy (EXAFS). EXAFS data analysis was performed with the Cumulant Method. For the crystalline-to-amorphous transformation, a progressive increase in bond-length was observed without the presence of an asymmetry in interatomic distance distribution (RDF). Beyond the amorphization threshold the RDF was dose dependent and asymmetric, where the bond-length and asymmetry increased as functions of ion dose. Such an effect was attributed to the formation of three- and five-fold coordinated atoms within the amorphous phase. Low-temperature thermal annealing resulted in structural relaxation of the amorphous phase as evidenced by a reduction in the centroid, asymmetry and width of the RDF, as consistent with a reduction in the fraction of non four-fold coordinated atoms. The results have been compared to other EXAFS studies of amorphous Ge, and it is suggested that the range of bond-lengths reported therein is related to the sample preparation method and state of relaxation.

Keywords: Extended X-ray absorption fine structure spectroscopy, amorphous Germanium, ion implantation.

1. Introduction

Despite many years of intensive research, a detailed understanding of the structure of amorphous materials is still lacking. For example, it is unclear whether differences in the structural properties of amorphous semiconductors prepared under varying conditions are artefacts of the preparation methodology or indicative of a continuum of metastable structural states. Structural relaxation of amorphous semiconductors (Donovan *et al.*, 1985, Fortner & Lannin, 1988, Roorda *et al.*, 1991) has also been studied to understand the micro-structural nature of this process. Though it was concluded that relaxation was due to annihilation of point defects in the amorphous phase, a model incorporating bond-angle re-ordering is equally appropriate. Annihilation of point defects would necessarily involve changes in bond-angles and bond-lengths in the local vicinity of the relaxation event. EXAFS is a technique very sensitive to the first nearest neighbour environment (1NN) (Filipponi & Di Cicco, 1995), and is able to provide information about even small changes in the bond-length distribution associated with relaxation (Bouldin *et al.*, 1991).

The goal of the present work was to determine the nature of implantation-induced structural modification in Ge and the effect of structural relaxation. The implantation-induced crystalline-to-amorphous transformation was investigated, and thereafter, further implantation-induced structural changes to the amorphous phase were characterized.

2. Experimental

We have utilized the ion-implantation processing methodology described in (Ridgway *et al.*, 1998) to prepare void-free, homogenous Ge films for EXAFS measurements. ⁷⁴Ge self implantations were performed at -196 °C, and 7° incidence. A multiple-energy, multiple-dose MeV implantation sequence was utilised to produce a near-constant distribution of energy deposition in vacancy production over depths of ~0.2-2.2 μm. A low ion flux was utilized to avoid beam-induced heating. Selected samples were relaxed by annealing at 200 °C for 1 hr in a N₂ ambient.

Transmission EXAFS measurements at the Ge K-edge were performed at 10 K on beamlines 2-3 and 4-3 of the Stanford Synchrotron Radiation Laboratory and 20-B of the Photon Factory. The EXAFS data was extracted from an absorption spectrum in the conventional manner (Sayers & Bunker, 1988). Analysis was performed with the Cumulant method (Bunker, 1983). Relative energy-scale calibration was achieved by aligning each absorption edge to within 0.1 eV. The energy origin ($E0$) was set at the maximum of the absorption-edge first derivative (Dalba *et al.*, 1995). The k^3 -weighted EXAFS data (where k is the photoelectron momentum) was Fourier transformed (FT) over the k range 2-18 Å⁻¹ using a 5% Hanning window. The back-transform was calculated using an R-space 20% Hanning window in the range 1.77-2.58 Å. The Fourier filtering process allowed direct extraction of the separate amplitude ($A(k)$) and phase ($\Phi(k)$) of the first-shell data used in the cumulant expansion.

The Cumulant method (Bunker, 1983, Dalba *et al.*, 1995) is a model-independent technique based on the expansion of EXAFS amplitudes and phases as a series of cumulants of the interatomic distance distribution. The EXAFS amplitudes and phases of the implanted samples (s) were compared to that of a known reference (r), in this case a crystalline sample. The difference in the cumulants $\Delta C1$ and $\Delta C3$ (where $\Delta Ci = Ci_s - Ci_r$) were obtained from a fit to the phase difference (Eqn. 1), and $\Delta C0$, $\Delta C2$ and $\Delta C4$ from a fit to the logarithm of the amplitude ratio (Eqn. 2):

$$\Phi_s(k) - \Phi_r(k) = 2k\Delta C1 - \frac{4}{3}k^3\Delta C3 + \dots \quad (1)$$

$$\ln \frac{A_s}{A_r} = \ln \frac{N_s}{N_r} + \Delta C0 - 2k^2\Delta C2 + \frac{2}{3}k^4\Delta C4 + \dots \quad (2)$$

Absolute magnitudes for the sample cumulants were obtained from the reference cumulants of the crystalline spectra, the latter determined assuming a Gaussian interatomic distance distribution. The electron mean free path, λ , was set equal to 5 Å independent of k , and the structural parameters were then obtained from Eqns. 3 and 4:

$$\Delta C0 = -2 \frac{\Delta C1}{\lambda} - 2(\ln C1_s - \ln C1_r) \quad (3)$$

$$R_s = C1 + \frac{2C2}{C1} \left(1 + \frac{C1}{\lambda} \right) \quad (4)$$

Specifically, $C0$ is a normalisation factor, $C1$ is related to R_s (the centroid of the RDF), $C2$ is the mean square displacement of the backscattering atoms to absorbing atoms (the Debye-Waller factor, σ^2), $C3$ measures asymmetry of the interatomic distance distribution, and $C4$ is connected to the symmetric width and shape of the distribution. The real interatomic distance distribution was determined from the FT of the reconstructed characteristic function in the range $|k| \leq 25 \text{ \AA}^{-1}$.

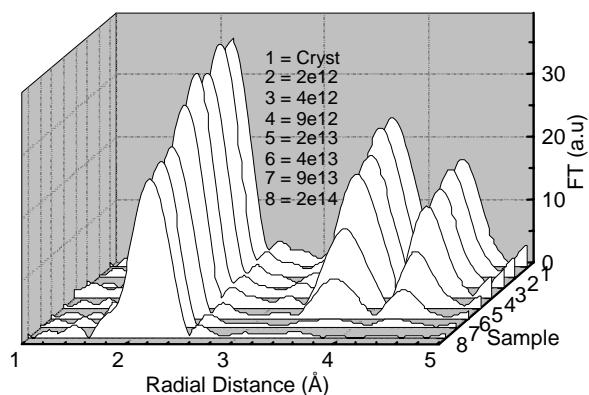


Figure 1
Fourier-transformed EXAFS spectra for the implantation-induced crystalline-to-amorphous transformation in Ge.

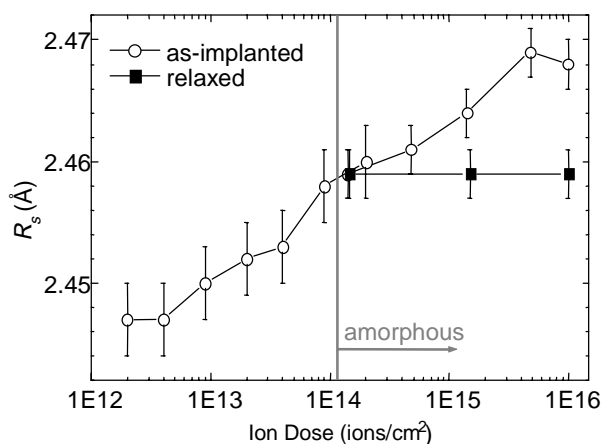


Figure 2
Nearest-neighbour a-Ge bond-length, R_s , as a function of ion dose for as-implanted and relaxed samples. The approximate amorphization threshold is denoted by the grey line.

3. Results

Shown in Figure 1 are the Fourier-transformed k^3 -weighted EXAFS spectra as a function of dose for the implantation-induced crystalline-to-amorphous transformation. The loss of crystalline order with increasing ion dose is readily apparent. Specifically, a reduction in amplitude and broadening of the 1NN peak can be attributed to a decrease in the short-range order about each Ge

absorber atom, as a result of bond-length distortions. No change was measurable in the 1NN coordination number from four atoms, indicative of the retention tetrahedral bonding character. The reduction and broadening of the second (2NN) and third (3NN) nearest neighbour peaks relate to loss of medium range order, through both bond-length and bond-angle distortions from those of unimplanted material. At and beyond the threshold dose for amorphization ($\sim 1e14 \text{ ions/cm}^2$), only a single peak (1NN) characteristic of the amorphous state is apparent.

Figure 2 shows the dose dependence of the bond-length, R_s , for an ion dose range spanning four orders of magnitude. Note that the bond-length increased continuously (within experimental error) from that of crystalline material, consistent with the presence of increasing structural disorder. At the amorphization threshold, the bond-length was $2.459 \pm 0.002 \text{ \AA}$. For ion doses beyond the amorphous threshold, R_s continued to increase. This is clear evidence of implantation-induced structural evolution *within* the amorphous phase. At the amorphization threshold, no asymmetry in the interatomic distance distribution was measurable (ie. $C3=C4=0$) or equivalently, the distribution was Gaussian. Beyond the amorphization threshold $C3$ increased with ion dose (Ridgway *et al.*, 2000). The interatomic distance distribution was reconstructed (Dalba *et al.*, 1995) for selected samples. The increased bond-length was manifested by an increased proportion of bond-lengths of value greater than the most probable value, yielding the readily apparent asymmetry in the RDF.

The observed trends in structural evolution were entirely consistent with an implantation-induced increase in the fraction of defective interatomic configurations. For the crystalline-to-amorphous transformation the creation and accumulation of both point and more complicated defects leads to amorphization either by the overlap of disordered regions or by a spontaneous collapse to the amorphous state once a threshold in stored energy is exceeded (see (Glover *et al.*, 2000) and Refs. therein). Our data support the former scenario, with the progressive increase in R_s related to the increase in residual disorder. *Ab-initio* molecular-dynamics calculations of amorphous Ge (Kresse & Hafner, 1994) have predicted the existence of three-, four- and five-fold coordinated atoms. The three- and five-fold coordinated atoms in the amorphous phase may be envisaged as analogues to crystalline point defects - a vacancy and interstitial, respectively. Their presence, with bond-lengths of 2.52 and 2.57 \AA respectively, exceeding that of the tetragonal site (2.47 \AA), would produce and a dose-dependant increase in bond-length, as observed. This is considered evidence for the dose-dependant increase of defective configurations *within* the amorphous phase.

The reconstructed RDF for structurally relaxed a-Ge (Glover *et al.*, 2000) is shown in Fig 3. Readily apparent in the inter-atomic distance distribution was a reduction in R_s , σ^2 and asymmetry. For all samples, thermally-induced relaxation at a temperature of 200 $^\circ\text{C}$ yielded a common bond-length value of $2.459 \pm 0.002 \text{ \AA}$ independent of initial dose. However, no change in R_s or σ^2 values (the latter not shown) were observed upon relaxation of the $1.4e14 \text{ ions/cm}^2$ sample. These suggest that structural relaxation does in fact proceed by the removal of point-like defects. The above argument equally applies to amorphous Ge produced by other techniques - it is the non-equilibrium nature of the amorphous phase formation process that determines the defect content (or metastability) of the network.

Many significant EXAFS studies of a-Ge exist (see eg. (Dalba *et al.*, 1995) (Filipponi & Di Cicco, 1995) and Refs. therein). Amorphous Ge bond-lengths have been reported in the range 2.45 – 2.47 \AA , with an asymmetric RDF in selected studies. Our results show that a range of bond-lengths (and asymmetry) are appropriate

for a-Ge, as the structural parameters are sensitive to the conditions of formation and the state of relaxation. Further, based on the results presented herein we suggest that relaxed a-Ge has a bond-length of $2.459 \pm 0.002 \text{ \AA}$, with a symmetric RDF.

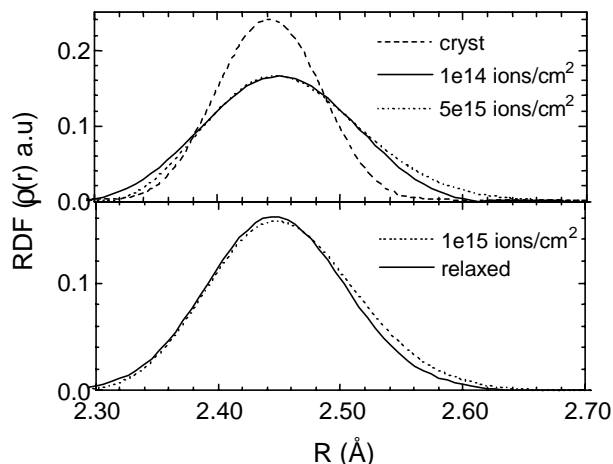


Figure 3

Real inter-atomic distance distribution for a pair of nearest-neighbour atoms as a function of ion dose. Also shown is the effect of relaxation for 1 hr at $200 \text{ }^\circ\text{C}$.

4. Conclusion

EXAFS has been used to characterize atomic-scale structural modifications in Ge produced by ion implantation. The interatomic distance distribution was shown to *continuously evolve* as a function of ion dose for the crystalline-to-amorphous transformation and for ion doses beyond the amorphization threshold. We suggest the micro-structural modifications in a-Ge resulted from an implantation-induced increase in the three- and five-fold coordinated atom fractions and represented a mechanism of accommodating vacancies and interstitials within the amorphous phase. Subsequent structural relaxation produced changes in the RDF as attributed to a reduction of the three- and five-fold coordinated atom fractions, thus supporting a model for relaxation via point-defect annihilation.

Acknowledgments

CJG, MCR and GJF were supported by the Australian Synchrotron Research Program, funded by the Commonwealth of Australia via the Major National Research Facilities Program. KMY is supported by the Department of Energy, Office of Basic Energy Sciences. ANL and JLH are supported by the Danish Natural Scientific Research Council. Work done (partially) at SSRL which is operated by the Department of Energy, Office of Basic Energy Sciences.

References

- Bouldin, C. E., Forman, R. A., Bell, M. I. & Donovan, E. P., (1991). *Phys. Rev. B*, **44**, 5492-5496.
- Bunker, G. (1983). *Nucl. Instrum. Methods* **207**, 437-444.
- Dalba, G., Fornasini, P., Grazioli, M. & Rocca, F., (1995). *Phys. Rev. B*, **52**, 11034-11043.
- Donovan, E. P., Spaepen, F., Turnbull, D., Poate, J. M. & Jacobson, D. C., (1985). *J. Appl. Phys.* **57**, 1795.
- Filippini, A. & Di Cicco, A., (1995). *Phys. Rev. B*, **51**, 12322-12336.
- Fortner, J. & Lannin, J. S., (1988). *Phys. Rev. B*, **37**, 10154-10158.
- Glover, C. J., Ridgway, M. C., Byrne, A. P., Yu, K. M., Foran, G. J., Clerc, C., Hansen, J. L. & Nylandsted-Larsen, A., (2000). *Nucl. Instrum. Meth. B*, **161-163**, 1033-1037.
- Glover, C. J., Ridgway, M. C., Yu, K. M., Foran, G. J., Desnica-Frankovic, D., Clerc, C., Hansen, J. L. & Nylandsted-Larsen, A., (2000). *Phys. Rev. B*. Accepted for publication.
- Kresse, G. & Hafner, J., (1994). *Phys. Rev. B*, **49**, 14251-14269.
- Ridgway, M. C., Glover, C. J., Tan, H. H., Clark, A., Karouta, F., Foran, G. J., Lee, T. W., Moon, Y., Yoon, E., Hansen, J. L., Nylandsted-Larsen, A., Clerc, C. & Chaumont, J., in *Applications of Synchrotron Radiation to Materials Science*, edited by S. Mimi, D. Perry, S. Stock, and L. Terminello (Materials Research Society, Pittsburgh, 1998), Vol. **524**, 309-312.
- Ridgway, M. C., Glover, C. J., Yu, K. M., Foran, G. J., Clerc, C., Hansen, J. L. & Nylandsted-Larsen, A., (2000). *Phys. Rev. B*, **61**, 12586-12589.
- Roorda, S., Sinke, W. C., Poate, J. M., Jacobson, D. C., Dierker, S., Dennis, B. S., Eaglesham, D. J., Spaepen, F. & Fuoss, P., (1991). *Phys. Rev. B*, **44**, 3702-3725.
- Sayers, D. E. & Bunker, B. A., in *X-Ray Absorption: Principles, Applications and Techniques of EXAFS, SEXAFS and XANES*, edited by D. C. Koningsberger and R. Prins (Wiley, New York, 1988), 211-253.